Organic & Biomolecular Chemistry

Dynamic Article Links

Cite this: *Org. Biomol. Chem.*, 2011, **9**, 7571

www.rsc.org/obc

PAPER

Molecular recognition probes of solvation thermodynamics in solvent mixtures

Valeria Amenta,[a] Joanne L. Cook,[a] Christopher A. Hunter,*[a] Caroline M. R. Low[b] and Jeremy G. Vinter[c]

Received 5th July 2011, Accepted 15th August 2011
DOI: 10.1039/c1ob06083j

High-throughput UV-Vis experiments using four molecular recognition-based probes, made by the combination of two hydrogen bond acceptors, tri-n-butylphosphine oxide and *N*,*N*′-bis(2-ethylhexyl)acetamide, and two hydrogen bond donors, 4-phenylazophenol and 4-nitrophenol, were performed. The association constants for the 1 : 1 H-bond interaction involved in each probe system were measured in mixtures of a polar and non-polar solvent, di-n-hexyl ether and n-octane, respectively. Similar behaviour was observed for all four systems. When the concentration of the polar solvent was low, the association constant was identical to that observed in pure n-octane. However, once the concentration of the polar solvent exceeded a threshold, the association constant decreased linearly with the concentration of di-n-hexyl ether. Selective solvation in mixtures can be understood based on the competition between the multiple competing equilibria in the system. In this case, solvation thermodynamics are dominated by competition of the ether for solvation of H-bond donors. For the more polar solute, 4-nitrophenol, the selective solvation starts at lower concentrations of the polar solvent compared with the less polar solute, 4-phenylazophenol. Thus the speciation and hence the properties of systems containing multiple solutes and multiple solvents can be estimated from the H-bond properties and the concentrations of the individual functional groups.

Introduction

Understanding solvation is essential for the rational use of solvents and solvent mixtures in chemical processes.[1] The choice of solvent has a profound influence on solubility, the spectroscopic properties of solutes, the affinity and selectivity of intermolecular interactions, the rate and mechanism of chemical reactions, and processes like crystallisation. Solvation is a complex property of the system as a whole, which makes it a difficult phenomenon to tackle from first principles. A range of empirical descriptors have therefore been developed to aid in the choice of solvent for a particular application and to interpret the behaviour of chemical systems that are solvent dependent.[2] However, chemistry is usually carried out in solvent mixtures, where the combinatorial explosion in the number of possible solvent systems makes the empirical approach daunting.

For an ideal mixture of two solvents, a solute will be solvated by both components of the mixture in proportion to the composition of the bulk liquid and the behaviour is straightforward. In general, however, the solute will be preferentially solvated by one component of the mixture, and the extent of this preferential solvation will vary over the surface of the solute in a way that depends on the functional groups involved. Thus molecules in mixed solvents tend to have complicated solvent shells, where there is a distribution of solvation states that depends on the composition of the bulk solvent and the surface properties of the solute (Fig. 1). A molecular-level treatment of the details of all of the interactions in the solvation shell is therefore required

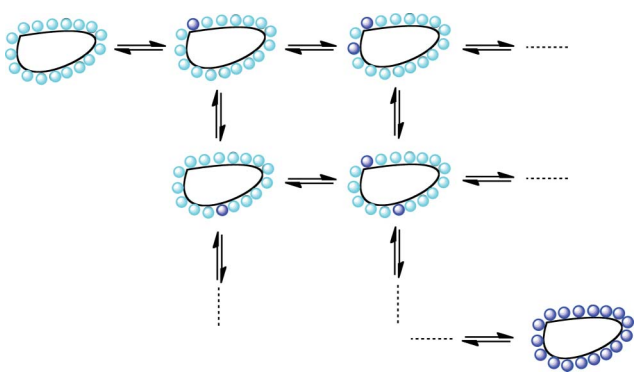

Fig. 1 When a solute is dissolved in a mixture of two different solvents, a large number of differently solvated species are present. The properties of the solute are determined by the Boltzmann-weighted population of all species.

[a]*Department of Chemistry, University of Sheffield, Sheffield, S3 7HF, UK. E-mail: c.hunter@shef.ac.uk; Fax: +44 (0)114 2229346; Tel: +44 (0)114 2229476*
[b]*Drug Discovery Facility, Rm 512 Biochemistry, Imperial College, London, SW7 2AY, UK*
[c]*Cresset Biomolecular Discovery, BioPark Hertfordshire, Broadwater Road, Welwyn Garden City, AL7 3A, UK*

to fully understand the consequences of preferential solvation phenomena.

A variety of spectroscopic probes have been used to study preferential solvation. These compounds usually have an NMR or UV/Vis absorption spectrum that changes in response to changes in the solvent environment.[3] Empirical parameters, like the equisolvation point, have been developed for characterizing solvation of these probes in binary solvent mixtures.[4,5] More detailed treatments are difficult, because in addition to changes in the local solvation shell, the bulk properties of a solvent mixture contribute to changes in spectroscopic properties observed in mixtures. Solvatochromic dyes are sensitive to overall solvent polarity, and NMR chemical shifts are sensitive to the bulk magnetic susceptibility. The COPS theory (competitive preferential solvation theory of weak molecular interactions) treats solvation in mixtures as equilibria involving both specific and non-specific interactions between the solutes and solvents. This approach has been applied to NMR and UV/Vis absorption studies of selective solvation as well as interpretation of reaction kinetics.[6,7]

Covington developed a thermodynamic treatment of preferential solvation of electrolytes in binary mixtures.[8] The solvation process is considered as a series of equilibria in which a molecule of one solvent is successively replaced by the other solvent (Fig. 1). The complexity of the multiple equilibria in these systems means that a number of assumptions and empirical parameters are required in order to apply the approach to experimental data, where there is usually only one spectroscopic observable. However, Engberts showed that the model could be used to interpret ^{1}H NMR data on preferential solvation of non-electrolytes in mixed aqueous solvents.[9] A similar solvent exchange model has been used to interpret UV/Vis data on the properties of solvatochromic dyes in binary solvent mixtures.[10]

Mass spectrometry has been used in an attempt to directly probe the composition of the solvation shell of solutes in binary solvent mixtures. In principle, this might allow characterisation of the populations of the different species illustrated in Fig. 1. Correlations have been observed between solvent organisation in the absence of solute and the composition of the solvation shell, but the observations do not provide a high-resolution picture of the multiple solvation states that are present.[11]

Our approach to the study of preferential solvation is based on the use of molecular recognition probes.[12] Instead of considering the solvent environment of the overall molecular surface, this approach focuses on the effect of the solvent on a single solute–solute hydrogen bonding interaction (Fig. 2)[13] and provides us with a very different point of view on the preferential solvation phenomenon. Thermodynamic measurements of solute–solute binding interactions are directly related to the populations of different solvation states and well-defined solvation equilibria involving just one site on the surface of each binding partner. We showed previously that the thermodynamics of solvation in mixtures can be understood at the molecular level based on the polarity and on the concentrations of functional groups present in the solvent. We now show that this behaviour is general and independent of the specific molecular recognition probe used. Here we study hydrogen bonding interactions for four different probe systems in alkane–ether mixtures using high throughput UV/Vis titration experiments.

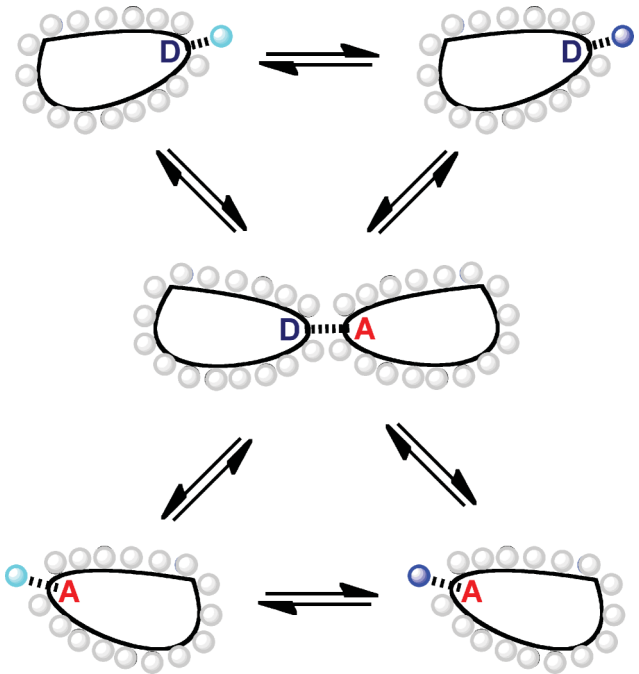

Fig. 2 Molecular recognition probes of solvation allow characterisation of interactions at individual binding sites on the solute surface. In a mixture of two solvents (dark blue and light blue), the behaviour of the system is determined by the thermodynamic properties of the five different species illustrated, providing a direct probe of selective solvation at the two binding sites A and D. Selective solvation at any of the other sites on the solute surfaces (grey) has little impact on the equilibria.

Results and discussion

Four combinations of two strong hydrogen bond donors, 4-phenylazophenol (**1**) and *p*-nitrophenol (**2**), and two strong hydrogen bond acceptors, tri-n-butylphosphine oxide (**3**) and *N*,*N*′-bis(2-ethylhexyl)acetamide (**4**) were used as molecular recognition probes of solvation equilibria (Fig. 3). These compounds are all sufficiently polar to form stable H-bonded complexes in competitive solvents like di-n-hexyl ether. The differences between the H-bond donor properties of **1** and **2** (α = 4.3 and 4.7, respectively) and the H-bond acceptor properties of **3** and **4** (β = 10.2 and 8.5, respectively) means that the stabilities of each of the four complexes differ significantly: by more than an order of magnitude in n-octane.[14–17] This system therefore allows us to explore the relationship between solvation equilibria in solvent mixtures and the properties of the solutes. Compounds **1–3** are commercially available, and **4** was prepared in one step from the corresponding acid chloride and amine.

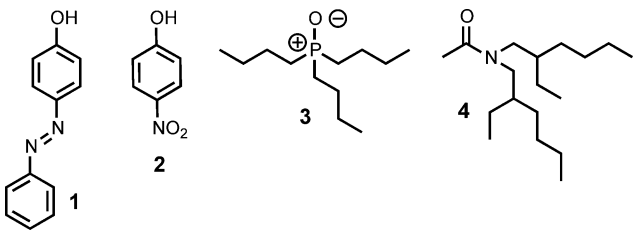

Fig. 3 H-bond donors, **1** and **2**, and H-bond acceptors, **3** and **4**, used in this study.

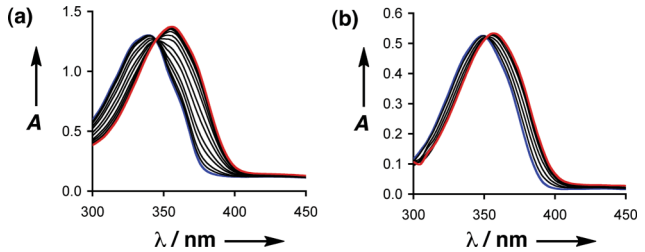

Fig. 4 UV/Vis absorption spectra for titration of **3** into **1** (a) in n-octane, **[1]** = 50 μM and (b) in di-n-hexyl ether, **[1]** = 20 μM. The spectra of the unbound **1** is shown in blue and of the **1**·**3** complex in red.

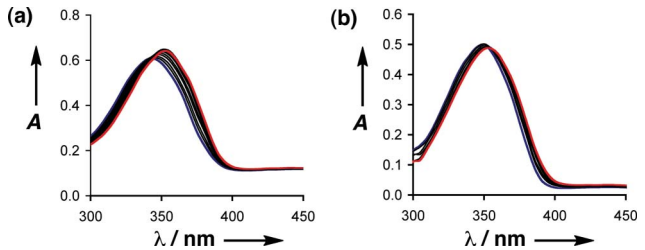

Fig. 5 UV/Vis absorption spectra for titration of **4** into **1** (a) in n-octane, (**[1]** = 20 μM) and (b) in di-n-hexyl ether, (**[1]** = 20 μM). The spectrum of unbound **1** is highlighted in blue and the **1**·**4** complex is highlighted in red.

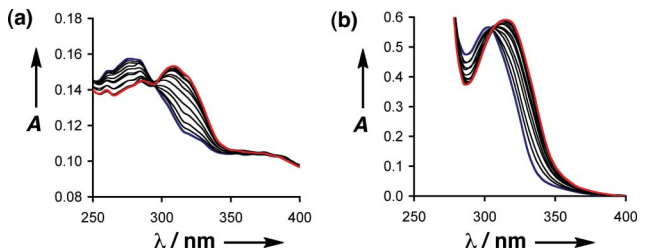

Fig. 6 UV/Vis absorption spectra for titration of **3** into **2** (a) in n-octane, (**[2]** = 5 μM) and (b) in di-n-hexyl ether (**[2]** = 49 μM).

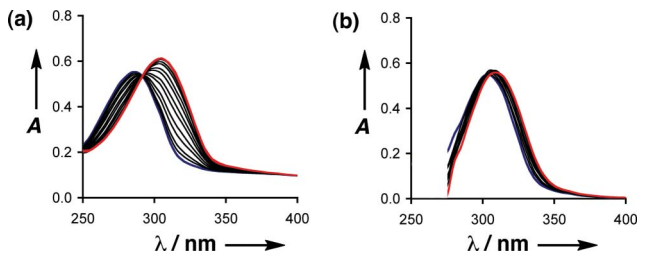

Fig. 7 UV/Vis absorption spectra for titration of **4** into **2** (a) in n-octane, (**[2]** = 50 μM) and (b) in di-n-hexyl ether (**[2]** = 46 μM). The spectrum of unbound **2** is shown in blue and the **2**·**4** complex in red.

Both **1** and **2** have strong UV/Vis absorption bands, which are sensitive to H-bonding interactions with the hydroxyl groups. The absorption maximum of **1** changes from 339 nm in n-octane to 349 nm in di-n-hexyl ether, due to the phenol–ether H-bond (Fig. 4). However, addition of **3** leads to a further shift in the absorption maximum to 356 nm, which is characteristic of the **1**·**3** complex and independent of the solvent (Fig. 4). Similarly if **4** is added, the absorption maximum of **1** shifts to 355 nm both in n-octane and in di-n-hexylether, due to the formation of the **1**·**4** complex (Fig. 5). H-bond donor **2** has an absorption maximum at 280 nm in n-octane, which changes to 300 nm in di-n-hexyl ether, due to the phenol–ether H-bond (Fig. 6). The **2**·**3** and the **2**·**4** complexes have absorption maxima at 315 nm and 305 nm, respectively, and these are also independent of the solvent (Fig. 6 and 7).

The phenolate anions obtained by deprotonation of **1** and **2** absorb at 420 nm and 405 nm, respectively (Fig. 8). The UV/Vis absorption spectra show no evidence for the presence of these species in any of the titration experiments described here, so the changes in the spectra in Fig. 4–7 can be ascribed to H-bond interactions between neutral species. No self-interaction process was observed for any of the compounds in ^{31}P NMR and UV/Vis dilution experiments, and the titration data for all four complexes both in n-octane and in di-n-hexyl ether fit well to a 1 : 1 binding isotherm. The corresponding association constants are listed in Table 1. The association constants vary from 10^3 to 10^6 M^{-1} in n-octane and from 10 to 10^3 M^{-1} in di-n-hexyl ether.

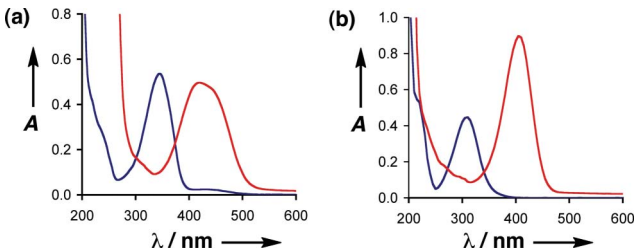

Fig. 8 (a) UV/Vis absorption spectra of **1** in acetonitrile (blue) and after addition of 100 μL of a 1 M solution of NaOH (red). (b) UV/Vis absorption spectra of **2** in acetonitrile (blue) and after addition of 100 μL of a 1 M solution of NaOH (red).

Automated titrations were also carried out using a UV/Vis plate reader, and the results are compared with the manual titrations in Table 1. The automated experiment could not be used to measure the association constant of the **2**·**3** complex in n-octane, because the stability of this complex is high and the extinction coefficient of **2** is low. At the μM concentrations of **2** that are required to measure an association constant of 10^6 M^{-1}, the absorption of **2** is not sufficient to obtain reliable titration data from the plate reader, which is less sensitive than a conventional spectrometer. For all of the other complexes, the results of the automated and manual experiments are identical within error, and so the automated system was used to collect titration data in mixtures of n-octane and di-n-hexyl ether.

We have previously reported on the properties of the **1**·**4** complex in a wide range of different alkane–ether solvent mixtures.[15] The results of this study showed that, above a certain threshold of

Table 1 Association constants measured by manual (log K_{man}/M^{-1}) and automated (log K_{auto}/M^{-1}) UV/Vis titration experiments at 298 K

	Solvent			
	n-octane		di-n-hexylether	
Complex	log K_{man}	log K_{auto}	log K_{man}	log K_{auto}
1·**3**	5.1 ± 0.2	5.0 ± 0.7	2.7 ± 0.2	2.6 ± 0.1
1·**4**	3.0 ± 0.1	3.2 ± 0.2	1.2 ± 0.1	0.9 ± 0.4
2·**3**	6.0 ± 0.3	—[a]	3.2 ± 0.1	3.0 ± 0.1
2·**4**	4.2 ± 0.1	4.1 ± 0.1	1.6 ± 0.2	1.5 ± 0.1

[a] This complex is too stable for reliable determination of log K using the automated experiment.

ether concentration, the value of log K is a linear function of the concentration of ether oxygen functional groups present in the mixture. Fig. 9 shows that this behaviour is common to all four molecular recognition probes. At low concentrations of di-n-hexyl ether, the stabilities of the complexes are identical to those in pure n-octane. Once the concentration of di-n-hexyl ether is sufficient to compete effectively with the alkane for solvation of the solutes, the stabilities of the complexes drop as a linear function of ether concentration.

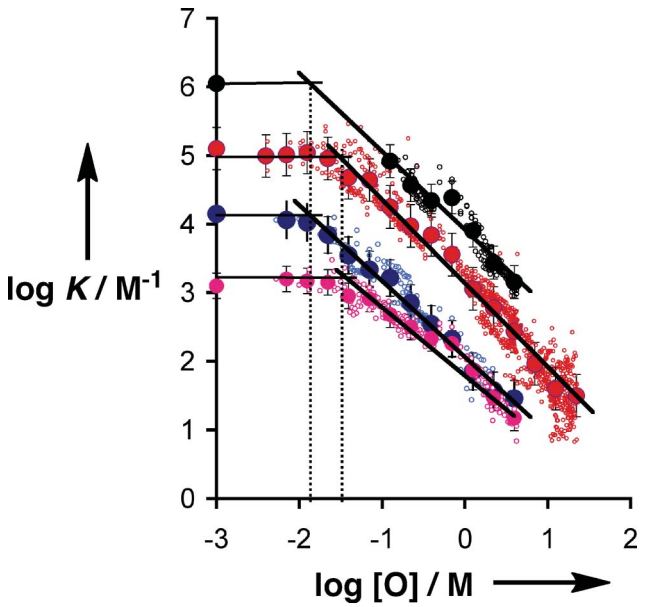

Fig. 9 Relationship between the association constants for the **1**·**3** (red), **1**·**4** (pink), **2**·**3** (black) and **2**·**4** (blue) complexes, log K, and the concentration of ether oxygen in the solvent mixture [O] for alkane–ether mixtures. Open circles are the results of the individual experiments, filled circles are the average values over windows of 0.25 units on the log K and log [O] scales with error bars at the 95% confidence limit. The points plotted on the y-axis represent the log K values for pure n-octane. The solid lines are the best fit straight lines for the relevant concentration regimes. The dotted lines highlight the ether concentrations at which there is a change in slope from one solvation regime to another.

Fig. 9 shows that for the two data sets that have **1** as the hydrogen bond donor (red and pink points), di-n-hexyl ether starts to solvate the phenol at an ether concentration of about 34 mM (highlighted by the dotted line). Once the ether concentration exceeds this value, there is a uniform decrease in the stability of the complexes. The data follow a straight line with a slope of –1.2 for the **1**·**3** complex and of –1.0 for the **1**·**4** complex. Similarly for the two data sets that have **2** as the hydrogen bond donor (blue and black points), the association constant doesn't change until an ether concentration of 13 mM is reached (dotted line in Fig. 9). Once the ether concentration exceeds this value, there is a decrease in the association constant and the data follow a straight line with a slope of –1.1 for both the **2**·**3** and the **2**·**4** systems. These observations are consistent with the H-bond donor properties of the solutes: **1** is a weaker H-bond donor than **2**, so a higher concentration of ether is required to form the **1**·ether complex that competes with binding to the H-bond acceptors, **3** and **4**.

The solvation of **1** and **2** by di-n-hexyl ether can be studied independently by using di-n-hexyl ether as the guest in UV/Vis absorption titrations in n-octane. The association constants in n-octane (K_S) are 28 ± 4 M^{-1} for the **1**·di-n-hexylether complex and 63 ± 1 M^{-1} for the **2**·di-n-hexylether complex. Thus the point at which log K starts to decrease in Fig. 9 is the point at which the phenol is approximately 50% solvated by ether, *i.e.* $K_S[O] \approx 1$. For **1**, $K_S[O] = 63 \times 13 \times 10^{-3} = 0.8$ at the intersection point on Fig. 9, and for **2**, $K_S[O] = 28 \times 34 \times 10^{-3} = 1.0$ at the intersection point.

These results provide strong evidence that the behaviour illustrated in Fig. 9 is a result of selective solvation of the H-bond donor group in alkane–ether mixtures. If the same H-bond donor is used with different H-bond acceptors, the onset of selective solvation occurs at the same concentration of ether, *i.e.* the phenomenon is independent of the H-bond acceptor. However, the onset of selective solvation does depend on the H-bond donor. When a more polar H-bond donor is used, the concentration of ether required to solvate it decreases. Thus selective solvation is a function of the nature of the solutes as well as the nature of the solvents. Polar solutes are more selective in the their solvation than non-polar solutes, because they bind more strongly to the polar component of the solvent mixture.

In general, the properties of solvent mixtures can be understood as a series of coupled equilibria (Fig. 10). Solvation of solutes, D and A, is dominated by interactions with the most polar complementary sites on the solvent molecules. For a binary solvent mixture, we denote the H-bond donor sites on the solvents α1 and α2 and the H-bond acceptor sites β1 and β2. Although they may not be highly populated, we also consider unsolvated states, where the solute and solvent molecules make no interaction with the bulk solvent. This allows us to derive a relationship that describes the observed association constant for formation of the D·A complex, K, in terms of the composition of the solvent mixture (eqn (1)).

$$K = \frac{[\mathrm{D} \bullet \mathrm{A}]}{[\mathrm{D}]_f [\mathrm{A}]_f} \tag{1}$$

where $[D]_f$ and $[A]_f$ are the total concentrations of solute that are not H-bonded to one another.

$$\begin{aligned}[\mathrm{A}]_f &= [\mathrm{A}] + [\alpha 1 \bullet \mathrm{A}] + [\alpha 2 \bullet \mathrm{A}] \\ &= [\mathrm{A}]\left(1 + K_{\alpha 1}[\alpha 1] + K_{\alpha 2}[\alpha 2]\right)\end{aligned} \tag{2}$$

$$\begin{aligned}[\mathrm{D}]_f &= [\mathrm{D}] + [\mathrm{D} \bullet \beta 1] + [\mathrm{D} \bullet \beta 2] \\ &= [\mathrm{D}]\left(1 + K_{\beta 1}[\beta 1] + K_{\beta 2}[\beta 2]\right)\end{aligned} \tag{3}$$

where [D], [A], [α1], [α2], [β1] and [β2] are the concentrations of the unsolvated species, and $K_{\alpha 1}$, $K_{\alpha 2}$, $K_{\beta 1}$ and $K_{\beta 2}$ are the equilibrium

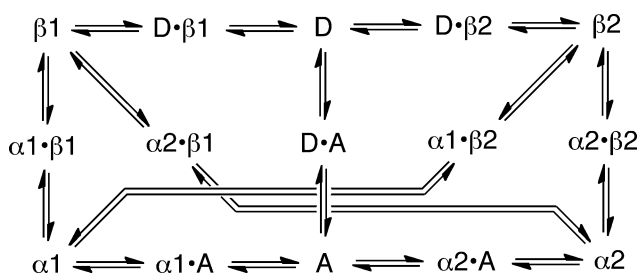

Fig. 10 Equilibria present in a mixture of two different solutes, A and D, dissolved in a mixture of two different solvents, 1 and 2. The species D, A, α1, α2, β1 and β2 represent unsolvated states.

constants for solvation of the solutes starting from unsolvated solute and unsolvated solvent.

Substitution into eqn (1) provides a relationship between the observed association constant, K, and a solvent independent equilibrium constant for formation of the D·A from unsolvated solutes, K_0 (eqn (4)).

$$K = \frac{[\mathrm{D}\bullet\mathrm{A}]}{[\mathrm{D}][\mathrm{A}]}\frac{1}{\left(1+K_{\beta 1}[\beta 1]+K_{\beta 2}[\beta 2]\right)\left(1+K_{\alpha 1}[\alpha 1]+K_{\alpha 2}[\alpha 2]\right)} = \frac{K_0}{\left(1+K_{\beta 1}[\beta 1]+K_{\beta 2}[\beta 2]\right)\left(1+K_{\alpha 1}[\alpha 1]+K_{\alpha 2}[\alpha 2]\right)} \quad (4)$$

In general, the concentrations of unsolvated solvent will change with solvent composition, and so the implementation of eqn (4) is not straightforward. However, for the system described in this paper, we have simplified the problem by choosing two solvents for which the H-bond donor properties are approximately invariant in mixtures. The solvent H-bond donors, α1 and α2, are CH groups with similar H-bond donor parameters (experimentally measured values of the H-bond donor parameter, α, are 0.9 for tetrahydrofuran and 1.1 for a variety of alkanes),[18,19] so the two sets of equilibrium constants involving the two different solvent H-bond donors are the same: $K_{\alpha 1} \approx K_{\alpha 2}$ which we will denote $K_{\alpha S}$. In addition, the concentrations of CH groups in n-octane and di-n-hexyl ether are identical: n-octane has 18 hydrogen atoms and a concentration of 6.16 M, and di-n-hexyl ether has 26 hydrogen atoms and a concentration of 4.26 M; [αS] = 111 M = [α1] = 18 × 6.16 = [α2] = 26 × 4.26.

Thus we can dramatically simplify eqn (4). Provided the solutes are present in sufficiently low concentrations that they do not perturb the populations of unsolvated solvent significantly, we can relate the concentrations of unsolvated solvent to the total concentrations of solvent present in the mixture.

$$[\beta 1]_0 = [\beta 1]+[\mathrm{D}\bullet\beta 1]+[\alpha 1\bullet\beta 1]+[\alpha 2\bullet\beta 1] \approx [\beta 1]\left(1+K_{S1}[\alpha S]\right) \quad (5)$$

where $[\beta 1]_0$ is the total concentration of oxygen H-bond acceptor sites, K_{S1} is the equilibrium constant for solvation of solvent β1 starting from unsolvated species and [αS] = [α1] + [α2], the total concentration of unsolvated solvent H-bond donors. Similarly,

$$[\beta 2]_0 \approx [\beta 2](1 + K_{S2}[\alpha S]) \quad (6)$$

where $[\beta 2]_0$ is the total concentration of alkyl H-bond acceptor sites.

When di-n-hexyl ether is added to n-octane, the maximum concentration of new H-bond acceptor groups that are introduced is 4 M (the concentration of neat di-n-hexyl ether). Since the total concentration of H-bond donor sites is 111 M, the value of [αS] cannot change by more than 4% over the entire concentration range, and so [αS], although unknown, can be treated as a constant. Similarly, we can assume that the concentration of alkyl H-bond acceptor sites is approximately constant in n-octane/di-n-hexyl ether mixtures, because the oxygen groups constitute a small fraction of the total solvent interaction sites even in pure di-n-hexyl ether. Thus eqn (4) can be rewritten as eqn (7).

$$K = \frac{K_0}{\left(1+\frac{K_{\beta 1}[\beta 1]_0}{1+K_{S1}[\alpha S]}+\frac{K_{\beta 2}[\beta 2]_0}{1+K_{S2}[\alpha S]}\right)\left(1+K_{\alpha S}[\alpha S]\right)} \quad (7)$$

The total concentration of oxygen H-bond acceptor sites $[\beta 1]_0$ is proportional to the concentration of di-n-hexyl ether, [S2], and all of the other parameters in eqn (7) are approximately constant. This provides a simple relationship between the observed association constant and the concentration of the solvent in the binary mixture.

$$K = \frac{a}{1+b[\mathrm{S2}]} \quad (8)$$

where a is the observed association constant in n-octane, $K_{D\cdot A}(S1)$, and b is the association constant for formation of the H-bond donor·di-n-hexyl ether complex in n-octane, $K_{D\cdot S2}(S1)$.

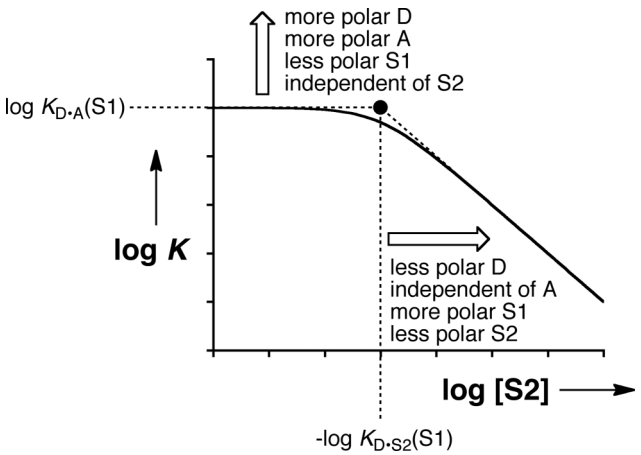

Fig. 11 Solvent dependence of the association constant, log K, for formation of a H-bonded complex, D·A, in mixtures of a non-polar solvent, S1, and a polar solvent, S2. The position of the horizontal dashed line is defined by the 1 : 1 association constant for formation of the D·A complex in S1, which depends on the polarity of D, A and S1, but is independent of S2. The position of the vertical dashed line is defined by the 1 : 1 association constant for formation of the D·S2 complex in S1, which depends on the polarity of D, S2 and S1, but is independent of A.

Fig. 11, which illustrates the relationship in eqn (8), closely resembles the experimentally determined profiles shown in Fig. 9. It is straightforward to predict the effects of changing the solute and solvent on the behaviour of the system from the constants, a and b. The onset of selective solvation is indicated by the black dot in Fig. 11, and the position of this point can be estimated from the association constants for formation of the A·D complex in S1 and for formation of the D·S2 complex in S1. Similar behaviour is expected for any system where one solvent, which contains a more polar functional group, is added to a less polar solvent. The association constants that correspond to the constants a and b in eqn (8) can be estimated using the relevant H-bond parameters and eqn (9).[14]

$$-RT\ln K = -(\alpha - \alpha_{S1})(\beta - \beta_{S1}) + 6\ \mathrm{kJ\ mol^{-1}} \quad (9)$$

where α is the H-bond donor parameter of the solute D or polar solvent S2, β is the H-bond acceptor parameter of the solute A

or polar solvent S2, and α_s and β_s are corresponding H-bond parameters of the non-polar solvent S1.

Thus it is possible to make quantitative predictions about the thermodynamic properties of solvent mixtures of this type and to construct theoretical versions of the profile in Fig. 11 for specific solute and solvent combinations. We will use the **2**·**4** complex to illustrate the approach with a worked example.

The value of the constant a in eqn (8) is the association constant for formation of the **2**·**4** complex in pure alkane. This association constant can be estimated using eqn (9). The H-bond donor parameter for **2** is $\alpha = 4.7$, and the H-bond acceptor parameter for 4 is $\beta = 8.5$.[14–17] The corresponding H-bond parameters for the alkane solvent are $\alpha_s = 1.0$ and $\beta_s = 0.6$.[18–19] Thus the value of a is given by eqn (10).

$$-RT\ln a = -(4.7 - 1.0)(8.5 - 0.6) + 6 \text{ kJ mol}^{-1} \quad (10)$$

This gives a value of $a = 1 \times 10^4$ M^{-1}, which is in good agreement with the experimental value in Table 1 ($\log K = 4.1 \pm 0.1 = \log a$) and defines the position of the horizontal part of the line in Fig. 11.

The constant b in eqn (8) is the association constant for formation of the **2**·ether complex in pure alkane. The H-bond donor parameter for **2** is $\alpha = 4.7$ as above, and the H-bond acceptor parameter for a dialkyl ether is $\beta = 5.3$.[14–17] The H-bond parameters for the alkane solvent are $\alpha_s = 1.0$ and $\beta_s = 0.6$ as above. Thus the value of b is given by eqn (11).

$$-RT\ln b = -(4.7 - 1.0)(5.3 - 0.6) + 6 \text{ kJ mol}^{-1} \quad (11)$$

This gives a value of $b = 1 \times 10^2$ M^{-1}. The vertical line drawn through the intersection point in the experimental data for the **2**·**4** complex in Fig. 9 is at $\log [O] = -1.9$. Thus the calculated value of $-\log b$ ($= -2.0$) accurately estimates the solvent concentration at which ether solvation starts to affect the observed association constant for formation of the **2**·**4** complex.

Thus for simple solvent mixtures, it is possible to make rather good quantitative predictions of solvent effects on complex stability using literature H-bond parameters for the functional groups involved. Deviations from the profile in Fig. 11 are expected if either or both solvents contain polar H-bond donors as well as acceptors, because all of the equilibria in Fig. 10 will be important in such systems. Data on the properties of these more complex solvent mixtures will be reported in due course.

Conclusions

The association constants for four different H-bonded complexes have been measured as a function of solvent composition for mixtures of an alkane, n-octane, and a more polar solvent, di-n-hexylether. This experiment provides a unique probe of the thermodynamics of selective solvation, because the association constant reports on the solvation of a single H-bond site on the surface of each solute. The four different complexes show similar overall behaviour. When the concentration of the polar solvent is low, the complexes have the same stability observed in the pure alkane. When the concentration of the polar solvent increases above a threshold, the ether begins to compete with the alkane for solvation of the H-bond donor, and the observed association constant falls as a linear function of the concentration of the polar solvent. This relationship is identical for all four complexes, but the onset of selective solvation by the more polar solvent is determined by the polarity of the solute. The strongest H-bond donor, 4-nitrophenol, interacts more strongly with the ether, and so selective solvation by the ether takes place at a lower concentration than observed for the less polar solute, 4-phenylazophenol.

These observations indicate that solvation properties of solvent mixtures can be understood simply based on the thermodynamic properties of discrete intermolecular contacts, and that the collective properties of the bulk liquid are of little significance. Competition between solvent–solvent and solvent–solute contacts leads to solvation thermodynamics that are system dependent, because the solute–solvent contacts change with the nature of the solute. However, the results imply that the behaviour of complex mixtures can be understood on the basis of the polarities and concentrations of the functional groups present. We note that the *solvation thermodynamics* discussed here are very different from the *solvation states* of the solutes. Once selective solvation by the more polar solvent exceeds 90%, the solvation state does not change much: the solutes are fully solvated by the more polar solvent, and this does not change as the concentration of polar solvent increases. In contrast, once the solutes are fully solvated by the more polar solvent, the solvation thermodynamics continue to change as the concentration of the polar solvent increases because of the influence of the solvent on the coupled equilibria illustrated in Fig. 10.

Experimental section

Synthesis of *N*,*N*′-bis(2-ethylhexyl)acetamide, 4

Tri-n-ethylamine (10 g, 99.4 mmol) was added to a stirred solution of bis(2-ethylhexyl)amine (20 g, 82.8 mmol) in dichloromethane (250 mL) under nitrogen. Acetyl chloride (7.8 g, 99.4 mmol) was added to the reaction mixture through a pressure-equalising dropping funnel. The reaction was quenched after 3 h with 250 mL of sodium hydroxide (10% solution), extracted with dichloromethane (5 × 50 mL), washed with HCl 0.1 M (200 mL), $NaHCO_3$ (2 × 200 mL) and 200 mL of brine. Then the organic layer was dried over sodium sulphate, filtered and concentrated *in vacuo* to give a pale yellow oil. The crude product was then purified by a reduced pressure distillation from barium oxide (fraction 1, 1 mBar, 140 °C) to yield a clear oil (16.4 g, 70%).

^{1}H NMR (250 MHz, $CDCl_3$): δ 3.18 (m, 4H), 2.05 (s, 3H), 1.62 (m, 2H), 1.23 (m, 16H), 0.85 (m, 12H). ^{13}C NMR (62.9 MHz, $CDCl_3$): $\delta = 170.84$, 52.13, 48.35, 38.31, 36.93, 30.50, 28.76, 23.89, 23.03, 21.95, 13.99, 10.80. MS (ES+) m/z (%) = 284 [M + H$^+$] (100), 325 (30); HRMS (Es+): calcd for $C_{18}H_{38}NO$: 284.2953; found 284.2941. FT-IR (thin film) ν_{max}/cm^{-1} 2954, 2922, 2857, 1644, 1458, 1422, 1378, 1233.

Manual UV/Visible absorption titrations

Manual titrations were carried out using a Cary 3 Bio UV-Vis spectrophotometer, using standard titration protocols. A 4 ml sample of the host (**1** or **2**) was prepared at a known concentration (0.005 mM to 0.05 mM). 0.7 ml of this solution was removed and added to a 1 ml quartz cuvette and the UV-Vis spectrum was recorded. The guest (**3** or **4**) was then dissolved in the remaining host solution to avoid dilution of the host during the titration.

Aliquots of guest solution were added successively to the cuvette containing the host solution, the cuvette was shaken, and the UV-Vis spectrum was recorded after each addition. The spectra were corrected for the guest absorption using independently determined extinction coefficients. The observed changes in UV-Vis absorption were analysed using a purpose-written fitting program in Microsoft Excel, and the data fit well to a 1 : 1 binding isotherm.

Automated UV/Vis absorption titrations

Association constants were determined using a BMG Labtech Fluorostar Optima and a BMG Labtech Fluorostar Omega plate reader with a Hellma 96-well quartz microplate. In a typical experiment, the microplate contained two titrations; the first in n-octane (S1) in wells 1–48 (titration 1), the second in di-n-hexyl ether (S2) in wells 49-96 (titration 2). In addition to mixtures of pure solvents, dilute solutions (10 vol %, 5 vol% and 2 vol %) of di-n-hexyl ether in n-octane were also used as S2. These solvent mixtures were prepared by volume. For example, a 2 vol % solution of di-n-hexyl ether in n-octane was prepared by transferring 2 mL of di-n-hexyl ether to a 100 mL volumetric flask, and the flask was then filled with n-octane. Two host stock solutions were prepared from accurately weighed samples of **1** or **2** (5 mg and 4 mg) dissolved in S1 and S2 in 25 mL volumetric flasks, to give a concentration of around 1 mM in each. Five guest stock solutions were prepared by dissolving an accurately weighed sample of guest in S1 or S2 in a 5 mL volumetric flask to give a 0.46 M stock solution of guest (stock solution 1). A serial dilution was carried out, whereby 570 μL of stock solution 1 was transferred to a 5 mL volumetric flask, which was then filled with S1 or S2 to give stock solution 2 (5.2×10^{-2} M). Each new stock solution was diluted in the same way to give a further three stock solutions, with concentrations of 6.0×10^{-3} M, 6.8×10^{-4} M and 7.7×10^{-5} M. However, in the experiments where the association constants were higher than 10^4 M^{-1} or 10^5 M^{-1}, 10 or 100 times more dilute guest solutions were used, respectively. Two sets of guest solutions were prepared, one in dissolved in S1, the other set dissolved in S2. These solutions were loaded onto the 96-well quartz microplate using four purpose written protocols with the UV/Vis plate reader. The first three protocols dealt with the pipetting of stock solutions of guest and host onto the microplate. The first protocol pipetted the two most dilute solutions of guest into wells 31–48, The next protocol pipetted the next two solutions of guest into wells 11–30, then the third protocol pipetted the most concentrated solution of guest into wells 1–10. Then 15 μL of a solution of host (1 mM) were pipetted into wells 1–48. This procedure was repeated for wells 49–96 (titration 2), using the stock solutions dissolved in S2. The final protocol was designed to top up each well with the relevant solvent to give a total volume of 150 μL in each well. There were repeats in some of the guest concentrations to highlight any possible errors in stock solution concentrations or pipetting. For example, wells 9 and 11 had the same concentration of 1. This was achieved by adding 15 μL of stock solution 1 to well 9 and 129 μL of stock solution 2 to well 11. The filling procedure was followed by addition of pure solvents to collect data for mixtures of S1 and S2. The absorbance of each well was measured at 6 wavelengths (260 nm, 280 nm, 340 nm, 390 nm, 420 nm and 600 nm) to obtain titration data in pure S1 and S2. After this, 10 μL aliquots of pure S2 were added into each well of titration 1 (dissolved in S1), and 10 μL aliquots of pure S1 were added into each well of titration 2 (dissolved in S2). After addition, the plate was agitated to ensure mixing, and then the instrument recorded the absorbance in each well. This procedure was repeated until all the wells were filled (320 μL), to give binding isotherms over the entire volume fraction range from pure S1 to pure S2.

The output is an Excel spreadsheet, which was analysed using the Solver routine to optimise a binding constant for each solvent composition (K), the extinction coefficient of the free host (ε_f), the extinction coefficient of the bound host (ε_b) and the extinction coefficient that describes the both guest absorbance and any secondary weak binding events (ε_A) to give a calculated absorbance (A_{calc}) that matches the experimental absorbance (A_{expt}). Dilution of the solutes during the solvent titration was taken into account in the analysis, but A_{expt} is not affected by this dilution, because there is a corresponding increase in the path length as the well is filled. The data was fit by minimising the sum of the residuals between A_{calc} and A_{expt} for every solvent composition in every well of the plate (eqn 12 and 13).

$$A_{calc} = \varepsilon_A[A] + \varepsilon_f[D]_f + \varepsilon_b[D]_b \quad (12)$$

$$[D]_b = \frac{1 + K[A]_0 + K[D]_0 - \sqrt{(1 + K[A]_0 + K[D]_0)^2 - 4K^2[A]_0[D]_0}}{2K} \quad (13)$$

where $[D]_b$ is the concentration of bound host, $[D]_f$ is the concentration of free host, $[D]_0$ and $[A]_0$ are the total concentrations of host and guest, respectively.

When the association constant is too low ($\log K < 2$), or too high ($\log K > 5$), the error in the automated experiments is significant. For the lower limit, this is due to the maximum guest concentration, which makes it impossible to reach saturation. For the upper limit, this is due to the host concentration, which must be low enough to avoid the tight binding limit ($[D] < 10/K$), but concentrated enough to have a detectable absorbance. For this reason the binding constant for the **2**·**3** complex in pure n-octane was determined only by manual UV/Vis titrations.

Acknowledgements

We thank the EPSRC for funding.

Notes and references

1 O. A. El Seoud, *Pure Appl. Chem.*, 2007, **79**, 1135–1151; Y. Marcus, *The Properties of Solvents*, John Wiley & Sons Ltd, England., 1998; C. Reichardt, *Solvents and Solvents Effects in Organic Chemistry*, 3rd. edn, WILEY-VCH Verlag GmbH & Co. KGaA, Weinheim (Germany), 2003.
2 A. R. Katritzky, M. Kuanar, S. Slavov, C. D. Hall, M. Karelson, I. Kahn and D. A. Dobchev, *Chem. Rev.*, 2010, **110**, 5714–5789.
3 Y. Marcus, *Solvent Mixtures Properties and Selective Solvation*, Marcel Dekker, Inc., New York, 2002.
4 L. S. Frankel, T. R. Stengle and C. H. Langford, *Chem. Commun. (London)*, 1965, **17**, 393–394.
5 L. S. Frankel and C. H. Langford, *J. Phys. Chem.*, 1970, **74**, 1376–1381.
6 O. B. Nagy, M. W. Muanda and J. B. Nagy, *J. Chem. Soc., Faraday Trans. 1*, 1978, **74**, 2210–2228.

7 M. W. Muanda, J. B. Nagy and O. B. Nagy, *Tetrahedron Lett.*, 1974, 3421–3424.
8 A. K. Covington in Vol. (Ed. K. E. Newman), Adv. Chem. Serv., 1976; A. K. Covington and K. E. Newman, *Pure Appl. Chem.*, 1979, **51**, 2041–2058.
9 K. Remerie and J. Engberts, *J. Phys. Chem.*, 1983, **87**, 5449–5455.
10 P. L. Silva, E. L. Bastos and O. A. El Seoud, *J. Phys. Chem. B*, 2007, **111**, 6173–6180.
11 F. Rastrelli, G. Saielli, A. Bagno and A. Wakisaka, *J. Phys. Chem. B*, 2004, **108**, 3479–3487.
12 J. L. Cook, C. A. Hunter, C. M. R. Low, A. Perez-Velasco and J. G. Vinter, *Angew. Chem., Int. Ed.*, 2008, **47**, 6275–6277.
13 J. L. Cook, C. A. Hunter, C. M. R. Low, A. Perez-Velasco and J. G. Vinter, *Angew. Chem., Int. Ed.*, 2007, **46**, 3706–3709.
14 C. A. Hunter, *Angew. Chem., Int. Ed.*, 2004, **43**, 5310–5324.
15 N. J. Buurma, J. L. Cook, C. A. Hunter, C. M. R. Low and J. G. Vinter, *Chem. Sci.*, 2010, **1**, 242–246.
16 M. H. Abraham, P. L. Grellier, D. V. Prior, P. P. Duce, J. J. Morris and P. J. Taylor, *J. Chem. Soc. Perkin Trans. 2*, 1989, 699–711.
17 M. H. Abraham, P. L. Grellier, D. V. Prior, J. J. Morris and P. J. Taylor, *J. Chem. Soc., Perkin Trans. 2*, 1990, 521–529.
18 R. Cabot and C. A. Hunter, *Org. Biomol. Chem.*, 2010, **8**, 1943–1950.
19 R. Cabot, C. A. Hunter and L. M. Varley, *Org. Biomol. Chem.*, 2010, **8**, 1455–1462.

